Materials Performance and Characterization

M. Czerner,[1] L. A. Fasce,[1] and P. M. Frontini[2]

DOI: 10.1520/MPC20130071

Wire Cutting Method to Assess Fracture Toughness of Gelatin Gels: Phenomenological Analysis and Limitations of Methodology

VOL. 3 / NO. 3 / 2014

Materials Performance and Characterization

doi:10.1520/MPC20130071 / Vol. 3 / No. 3 / 2014 / available online at www.astm.org

M. Czerner,[1] L. A. Fasce,[1] and P. M. Frontini[2]

Wire Cutting Method to Assess Fracture Toughness of Gelatin Gels: Phenomenological Analysis and Limitations of Methodology

Reference

Czerner, M., Fasce, L. A., and Frontini, P. M., "Wire Cutting Method to Assess Fracture Toughness of Gelatin Gels: Phenomenological Analysis and Limitations of Methodology," *Materials Performance and Characterization*, Vol. 3, No. 3, 2014, pp. 1–21, doi:10.1520/MPC20130071. ISSN 2165-3992[3]

Manuscript received October 8, 2013; accepted for publication November 25, 2013; published online January 17, 2014.

[1] Instituto de Investigaciones en Ciencia y Tecnología de Materiales (INTEMA), Universidad Nacional de Mar del Plata, CONICET, Av. J.B. Justo 4302, B7608FDQ, Mar del Plata, Argentina.

[2] Instituto de Investigaciones en Ciencia y Tecnología de Materiales (INTEMA), Universidad Nacional de Mar del Plata, CONICET, Av. J.B. Justo 4302, B7608FDQ, Mar del Plata, Argentina (Corresponding author), e-mail: pmfronti@fi.mdp.edu.ar

[3] This paper is a contribution to a Special Issue of *Materials Performance and Characterization* on "Fracture Toughness," Guest Editors, Bojan Podgornik and Votjeh Leskovsek, Institute of Metals and Technology, Ljubljana, Slovenia.

ABSTRACT

In this work the performance of the wire cutting method for determining the fracture toughness, G_c, of gelatin hydrogels is assessed. In this method, wires of different diameters are pushed into a sample while the force and displacement are continuously recorded. The cutting action reaches a steady state, in which fracture propagation, deformation, and friction occur simultaneously. The method implies a linear relationship between the steady-state cutting force per unit sample width and the wire diameter, of which the *y*-intercept is G_c. Several gel samples differing in gelatin concentration, source (bovine or porcine), solvent (water or water–glycerol mixture), and crosslink type (physical or chemical induced by glutaraldehyde) were tested at different rates. Post-mortem fracture surfaces examined via optical microscopy displayed four different morphologies depending on the gel formulation, cutting rate, and wire diameter: I, striated; II, with one or two oblique straight lines; III, with rhombus-like figures; and IV, with material pull-out. A direct relationship between the developed fracture surface morphology and the method performance existed. One necessary condition for obtaining the linear relationship is a unique fracture surface morphology remaining for all of the wires utilized in the determination. The method is invalid if the fracture surface morphology changes with changing wire diameter, abnormal crack path

deflection takes place, or material pull-out occurs as a result of adhesion effects. The applicability of the method seems to be not constrained to physical gels. An appropriate cutting rate and wire diameter have to be selected in order for a unique fracture surface morphology to be achieved. In such cases, reasonable G_c values were obtained from the *y*-intercept of the best linear fit of experimental data. G_c increased with increasing gelatin concentration, Bloom number, and solvent viscosity. Moreover, G_c was greater when a rhombus-like pattern was induced rather than other morphology due to greater crack path tortuosity.

Keywords

soft materials, gelatin gels, wire cutting method, fracture toughness

Introduction

To date, the mechanical testing of soft matter has focused primarily on deformation rather than failure properties. However, for novel engineering applications, mechanical integrity appears to be very important, and mechanical failure is ready to stand alongside stiffness as a functional design requirement. Therefore, the development of a fundamental understanding of and new methods with which to evaluate mechanical properties of soft materials such as fracture toughness is an attractive topic for the technical community.

Fracture of gels is a less established field of study—much less so than that of metals, ceramics, and polymers [1]. In recent years, several typical fracture mechanics test configurations such as SE(B), SE(T), DE(T), tear, wedge splitting, and cutting have been tried in an attempt to determine the fracture toughness of different soft material classes [2–7].

Specifically, the wire cutting method was proposed as a suitable methodology for determining the fracture toughness of cheeses [2,8,9] and starch hydrogels [10]. The most attractive feature of this methodology is its simplicity, and it is particularly easy to implement when testing self-supporting materials of very low stiffness. In previous studies [2,8–10], very good agreement between fracture parameters arising from standard fracture mechanics configurations [SE(B) and SE(T)] and wire cutting was found.

Conversely, Baldi et al. were not able to apply the wire cutting method to evaluate the fracture toughness of polyacrylamide (PAA) hydrogels [11], despite the fact that the stiffness of the gels was similar to that of cheeses and starch gels. Therefore, the general performance of the wire cutting method for fracture toughness determination in soft materials needs to be further explored in order for it to be deemed reliable. The limits of the methodology and the applicable experimental conditions also have to be well established.

In this work, the performance of the wire cutting methodology under different experimental conditions was assessed using gelatin hydrogels. These materials are appealing in that their structural features and mechanical properties can be easily tuned. In addition, their fracture behavior is of great importance because of their

applications in food, ballistic, and biomedical fields thanks to their unique functional, gelation, and biomimetic properties [12–16].

Gelatin is a mixture of polypeptide molecules obtained from the denaturation of collagen from different natural sources, mainly pig skin, bovine hide, and pork and cattle bones [12]. Gelatin is able to dissolve in aqueous solutions, where it exists as single coils. When the solution is cooled, a thermoreversible gel is obtained, thanks to the formation of a physical network that is constituted by triple helical collagen-like sequences (crosslinking points) interconnected by flexible protein chains. The gelatin network can be changed by chemical crosslinking using agents such as glutaraldehyde, carbodiimides, transglutaminase, or salts [17–19]. Gelatin gels' properties can also be modified by the incorporation of neutral co-solvents such as glycerol and sorbitol [19–21].

It was previously established that gelatin hydrogels display highly nonlinear elastic behavior [16,21,22], brittle fracture, and rate-dependent failure phenomena [5].

THE WIRE CUTTING METHOD

Theoretically, the cutting action of a wire is that of "separating by dividing" with no loss of material [23]. In the wire cutting method, wires of various diameters are pushed into the sample while the force and displacement are continuously recorded. In the analysis of the cutting process, it is assumed that a crack develops ahead of the wire. The process has two distinct phases: an initial indentation phase, in which the load increases with increasing wire penetration, and a steady-state cutting phase, in which the load remains almost constant (**Fig. 1**). At the beginning of the test, the wire deforms the material up to some point at which fracture is initiated. After that, the load falls down abruptly as a result of the release of the elastic energy stored in the sample by instantaneous crack propagation. Then, the cutting action reaches a steady-state stage. Fracture, deformation, and friction occur simultaneously in the steady-state cutting stage. Based on the energy balance, it has been stated that the

FIG. 1
Schematic representation of theoretical force–displacement curve registered in wire cutting experiments.

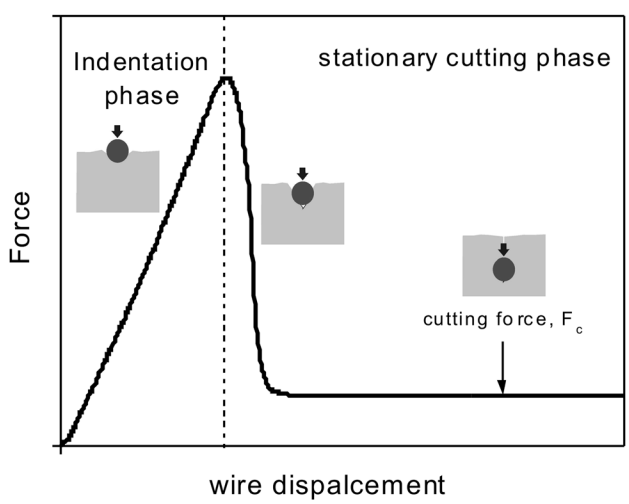

force required in order to sustain the cutting is proportional to the wire diameter d_w, and that there is a constant contribution arising from the fracture toughness G_c. The proportionality factor is related to energy-dissipative contributions such as viscous deformation and friction processes occurring at the interface between the wire and the sample material.

The following expression was proposed by Kamyab et al. [2] for the relationship between the cutting force F_c and the wire diameter:

$$\frac{F_c}{B} = G_c + (1+\mu)\sigma_y d_w \tag{1}$$

where:

B = sample width,

μ = kinematic friction coefficient, and

σ_y = a characteristic stress.

Equation 1 establishes a linear relationship between the cutting force per unit width and the wire diameter, of which the intercept is G_c.

The fracture toughness of a sample is then determined from the best linear fit of the recorded F_c/B values from tests performed with wires of different diameters.

Kamyab et al. [2] proved that this method was accurate for determining the fracture toughness of cheeses. This is a kind of soft material with an elastic modulus in the range of 100 to 350 kPa that exhibits brittle fracture and rate dependence. They demonstrated that the fracture toughness values obtained with the method compared well with those from SE(T) experiments.

Furthermore, Gamonpilas et al. [10] showed that the wire cutting method was also suitable for evaluating the fracture toughness of several starch hydrogels displaying an elastic modulus in the range of 50 to 200 kPa. They demonstrated that the values of G_c were in good agreement with those obtained from SE(B) tests and that G_c values increase with increasing cutting speed.

Unfortunately, in a recent work, Baldi et al. [11] found that the method of Eq 1 failed in evaluating the fracture toughness of PAA hydrogels, despite the fact that their samples exhibited brittle fracture behavior and an elastic modulus within the same range as those of the previously mentioned materials (50 to 300 kPa). Some differences between the testing conditions used in Baldi et al.'s work [11] and the ones in which the method was applied with success [2,9,10] existed: (i) the chemical nature of the crosslinks in the gel network of the tested samples, (ii) the lower cutting rate used, (iii) the uneven fracture propagation pattern that developed with some wire diameters, and (iv) the specimen configuration used (prenotched samples).

Inspired by these differences, some questions arise about the applicability of the wire cutting method in evaluations of soft materials: Is it constrained only to physical gels? Is it influenced by the cutting rate? Is it related to the fracture pattern?

To answer these questions and give insight into the wire cutting methodology, we prepared and tested several gelatin gels differing in gelatin concentration, gelatin source, solvent composition, and crosslink type at different cutting rates. A broad investigation of fracture phenomenology and the performance of the methodology is presented.

Experimental

MATERIALS AND SAMPLE PREPARATION

Gels exhibiting different structural and fracture behavior were prepared from type B gelatin (200 Bloom) from bovine hide (BoGe) and type A gelatin (250 Bloom) from pig skin (PoGe).

Physical gelatin gels of different powder concentrations (10 %, 20 %, and 30 % wt/wt), and thus different stiffnesses, were prepared. The gelatin powder was dissolved in a buffer solution selected over the gelatins' isoionic points using a hot plate stirrer and held at 50°C for 15 min. A chemically crosslinked gelatin gel was prepared by adding glutaraldehyde (GTA) (0.75 wt. % with respect to gelatin powder weight) to the 10 % wt/wt BoGe solution. In addition, glycerol (Gly) was incorporated into the 20 % wt/wt BoGe gel formulation at a concentration of 25 wt. % (based on dry gelatin powder).

Hot mixtures were poured into rectangular Delrin molds (25 mm width by 25 mm height by 40 mm length) previously lubricated with Teflon spray and then allowed to set for 1 h at room temperature. Gel samples were wrapped in film in order to minimize drying and stored at 4°C ± 1°C for 48 h. Before testing, samples were conditioned at 20°C ± 1°C for 2 h.

The samples' designation and composition are detailed in **Table 1**, together with the samples' gel strength values. Gel strength is a technological property associated with the sample's stiffness [13,24]. Values were determined in a way similar to the method used for the Bloom number (i.e., the force required to penetrate a cylindrical flat-ended indenter 4 mm into the sample), but at 20°C and with the actual composition of each gel sample [13].

The stiffnesses of the investigated samples were ranked as follows: BoGe-30 > PoGe-20 > BoGe-20 ≈ BoGe-20-Gly > BoGe-10-GTA > BoGe-10.

WIRE CUTTING TESTS

Wire cutting experiments were performed at 20°C ± 1°C in an INSTRON 4469 universal testing machine equipped with a specially designed grip and a 0.5-kN load cell. **Figure 2** shows a representative specimen and testing configuration. The grip allowed the wire to be pulled tight (wire pretension ~600 MPa) and perfectly aligned with the sample surface. Seven stainless steel orthodontic wires of different diameters (d_w) ranging from 0.2 to 0.8 mm were used. The cutting rate was varied from 0.5 to 100 mm/min.

TABLE 1

Sample designation, formulation, and gel strength of prepared gelatin hydrogels.

Sample Designation	Gel Composition	Gel Strength, N
BoGe-10	10 wt. % BoGe, buffer solution pH = 7	1.09 ± 0.06
BoGe-10-GTA	10 wt. % BoGe, buffer solution pH = 7, 0.75 % wt/wt$_{BoGe}$ GTA	1.34 ±0.02
BoGe-20	20 wt. % BoGe, buffer solution pH = 7	3.87 ±0.27
BoGe-20-Gly	20 wt. % BoGe, buffer solution pH = 7, 25 % wt/wt$_{BoGe}$Gly	3.61 ±0.24
BoGe-30	30 wt. % BoGe, buffer solution pH = 7	8.70 ±0.45
PoGe-20	20 wt. % PoGe, buffer solution pH = 10	4.56 ±0.36

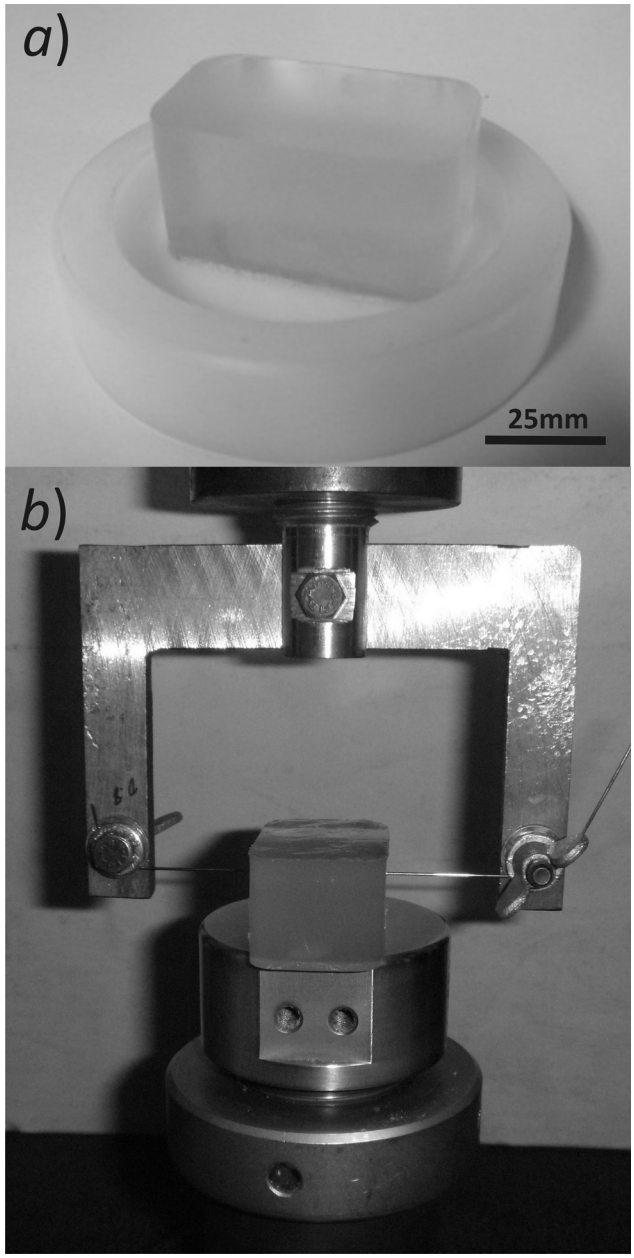

FIG. 2
Photographs showing (a) hydrogel specimen and (b) wire cutting test configuration.

At least five cuts were performed for each wire diameter. No more than five cuts were made on each block, according to Goh's results on cheese samples [8]. He found that the cutting curve is independent of the sample length when it is approximately ten times the wire diameter.

Special care was taken to note whether the wire appreciably deflected during testing. If wire deflection was noticeable, data were eliminated from the analysis, as the force–displacement acquired did not reflect the actual wire displacement into the

sample [8]. When it was not possible to keep the wires taut enough, prenotched specimens were used. This was the case for the stiffest gel samples and thinnest wires. The prenotch was introduced by sliding a razor blade along the cutting axis to a depth of about 2 mm. The existence of prenotching markedly reduced the maximum load achieved during the indentation phase and hence decreased the force sustained by the wire. This experimental strategy was proposed by Baldi et al. [11,25].

The post-mortem fracture surface morphology was examined via optical microscopy. Images were taken at a magnification of 20 × immediately after the cutting test was performed.

Results and Discussion

The influence of the cutting rate was explored through wire cutting experiments performed at different cutting rates (5, 25, and 100 mm/min) on gel samples prepared at different gelatin concentrations (BoGe-10, BoGe-20, and BoGe-30) and with different gelatin sources (BoGe-20 and PoGe-20). The influence of crosslink type in the gel network (physical and chemical) was analyzed using the experiments performed at 25 mm/min on GeBo-10 and GeBo-10-GTA samples. The effect of added glycerol (i.e., the effect of increased solvent viscosity) was investigated in GeBo-20 and GeBo-20-Gly samples at 5 and 25 mm/min. For all these experiments, the load–displacement curves were examined in light of the post-mortem fracture surfaces. Cutting rates of less than 5 mm/min were used only to investigate the macroscopic fracture surface morphology.

PHENOMENOLOGY: FRACTURE PATTERNS AND FORCE–DISPLACEMENT CURVES

Macroscopic Fracture Morphologies

Post-mortem fracture surfaces revealed the development of different macroscopic morphologies depending on the gel sample formulation, cutting rate, and wire diameter. Representative optical microscopy images of each type of morphology are shown in **Fig. 3**. These morphologies can be divided into four types:

I: striated surfaces with lines aligned parallel to the wire advance direction [**Fig. 3*(a)***]

FIG. 3 Optical microscopy images showing the different fracture surface morphologies observed in wire cutting experiments: (a) BoGe-10-GTA, V = 25 mm/min, d_w = 0.6 mm; (b) PoGe-20, V = 100 mm/min, d_w = 0.5 mm; (c) BoGe-20, 5 mm/min, d_w = 0.4 mm; and (d) BoGe-30, V = 25 mm/min, d_w = 0.5 mm.

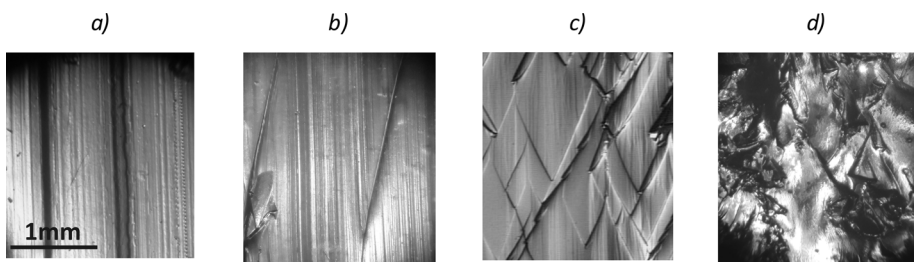

II: surfaces showing one or two straight lines oriented about 45° to the wire advance direction [**Fig. 3(*b*)**]

III: surfaces displaying regular rhombus-like structures, in which each quadrilateral figure is actually a step [**Fig. 3(*c*)**]

IV: surfaces displaying severe damage with material pull-out [**Fig. 3(*d*)**]

Post-mortem samples displayed two matching fracture surfaces for morphologies of types I, II, and III. The global fracture propagation direction coincided with the wire advance direction, but the existence of steps on the surfaces indicated that the crack actually propagated with a nonplanar crack front. Moreover, in the type III morphology, the crack front tilted and twisted regularly, leading to a crack path larger than the nominal one—that is, the roughness number used to describe the geometry of a surface in the macroscale was greater than unity.

The type IV morphology shown in **Fig. 3(*d*)** is a mixed pattern formed by a combination of types I, II, and III with highly stretched regions and pulled-out material. The pair of surfaces produced in one cut did not fit each other. The cause of the formation of this type of morphology seems to be the existence of adhesion between the wire and the sample material.

The following statements emerged from the analysis of the fracture surfaces observed in the different samples and tested conditions:

- The fracture surface morphology became striated rather than rhombus-shaped as the cutting rate was increased for the same gel composition and wire diameter, as exemplified in **Fig. 4**.
- The number of rhombus-like structures tended to decrease and their dimensions increased with increasing wire diameter for the same gel composition and cutting rate, as shown in **Fig. 5**. The crack tortuosity tended to decrease as the wire diameter increased.

FIG. 4 Optical microscopy images showing the transition from rhombus-like to striated fracture surface patterns with increasing cutting rate: BoGe-20, $d_w = 0.25$ mm at (a) 0.5 mm/min, (b) 1 mm/min, (c) 5 mm/min, and (d) 50 mm/min; BoGe-30, $d_w = 0.3$ mm at (e) 5 mm/min, (f) 25 mm/min, (g) 50 mm/min, and (h) 100 mm/min.

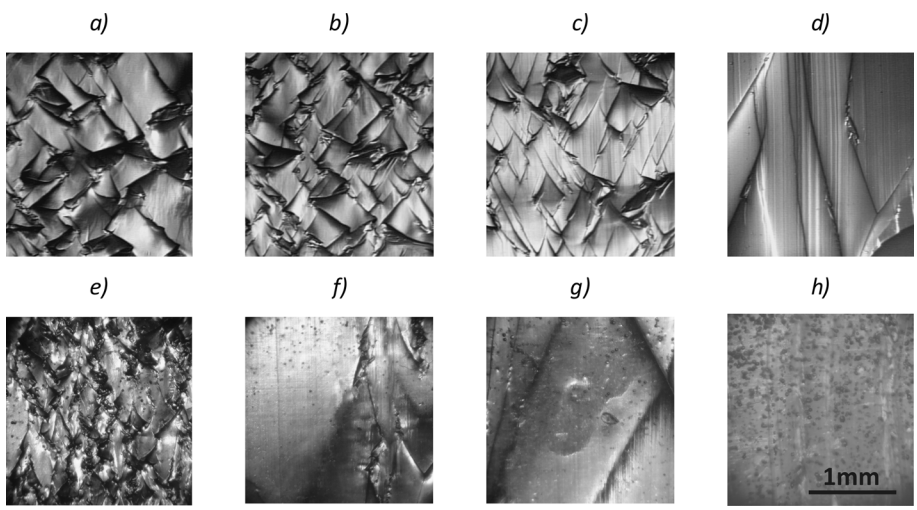

FIG. 5 Optical microscopy images showing changes in the fracture surface of rhombus-like morphology with increasing wire diameter: PoGe-20, 5 mm/min, (a) $d_w = 0.2$ mm, (b) $d_w = 0.4$ mm, (c) $d_w = 0.6$ mm, and (d) $d_w = 0.8$ mm.

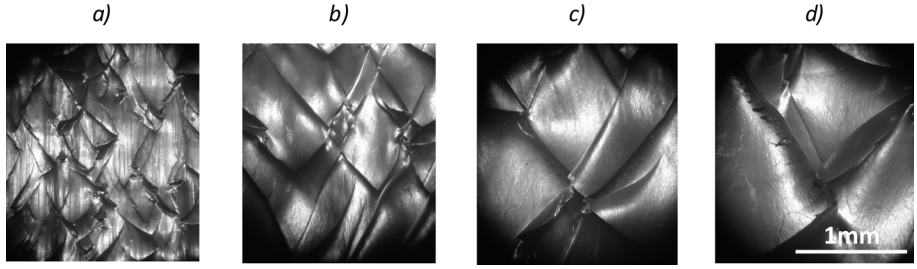

- In physical BoGe gels, the pattern dimensions of the rhombus-shaped morphology decreased with increasing gelatin concentration for the same cutting rate and wire diameter.
- Material pull-out was observed only on the fracture surfaces of the most concentrated gelatin gel samples (BoGe-30). In addition, at a constant cutting rate, pull-out damage increased with increasing wire diameter (**Fig. 6**).

Morphologies of types I, II, and III have been previously observed in chemical [11,26] and physical hydrogels [27], and also in elastomers [28]. Regular patterns similar to those of types I and III were first described by Tanaka et al. for fracture surfaces of PAA hydrogels induced by mode I crack opening [26]. They referred to them as a "river-like pattern" (type I) and a "scale pattern" (type III). They found that the fracture surface pattern changes from a river to a scale pattern with an increasing crack growth rate. Steps on surfaces were attributed to small mode-III-like regions created at the crack tip that propagate along the global propagation direction in the river pattern and at 45° in the scale-like pattern. Later, fracture surfaces in gelatin hydrogels were deeply investigated by Baumberger et al. [27]. They reported that at crack velocities greater than a critical value (V_c), the fracture surface appears flat on the macroscale but exhibits a microrough morphology, which was attributed to in- and out-of-plane deviations of the crack front line due to the randomness of the network structure. Below V_c, the fracture surface also displays oblique straight line defects oriented at a characteristic angle (about 43°) to the crack propagation direction (type II morphology) that proliferate into a "cross-hatched" morphology (identical to the scale pattern or our type III morphology) with a further reduction in velocity. They found that the characteristic angle is the same as the

FIG. 6 Optical microscopy images showing the particular fracture surface patterns observed in BoGe-30 samples with increasing wire diameter: V = 25 mm/min with (a) $d_w = 0.2$ mm, (b) $d_w = 0.4$ mm, (c) $d_w = 0.6$ mm, and (d) $d_w = 0.8$ mm.

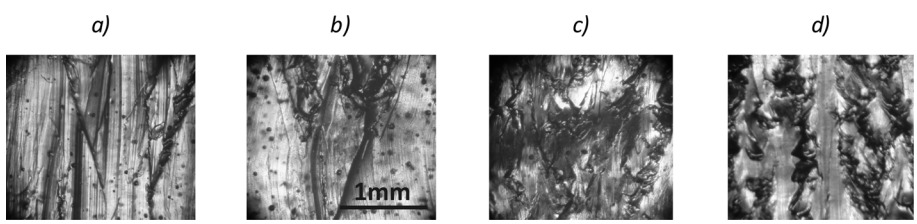

one observed in the microrough morphology, and it appears to be independent of the crack propagation velocity. Baldi et al. [11] described a similar rhombus-like pattern for a series of PAA hydrogels differing in polymer concentration (gel stiffness). It can be seen in their optical macrographs that in all samples the dimensions of the rhombus-like pattern increased with increasing wire diameter, and the crack tortuosity decreased (i.e., the magnitude of the out-of-plane crack front deflection was lower or the steps heights were shorter).

Force–Displacement Curves

The acquired force–displacement curves showed an indentation phase followed by a steady cutting one, in agreement with previous findings (**Fig. 1**). It was noted that a direct relationship existed between the macroscopic fracture surface morphology and the shape of the load–displacement curve, as shown in Figs. **7** through **9**.

When the fracture surface was striated or exhibited one or two oblique straight line defects, the part of the curve related to the cutting phase achieved a constant value [**Figs. 7(*a*)** and **7(*b*)**]. Conversely, when the fracture surface displayed rhombus-like structures, the force–displacement curve oscillated around a constant

FIG. 7 Typical load–displacement curves obtained in wire cutting experiments according to surface morphology: (a) BoGe-10-GTA, V = 25 mm/min, d_w = 0.6 mm; (b) PoGe-20, V = 100 mm/min, d_w = 0.5 mm; (c) BoGe-20, V = 5 mm/min, d_w = 0.25 mm.

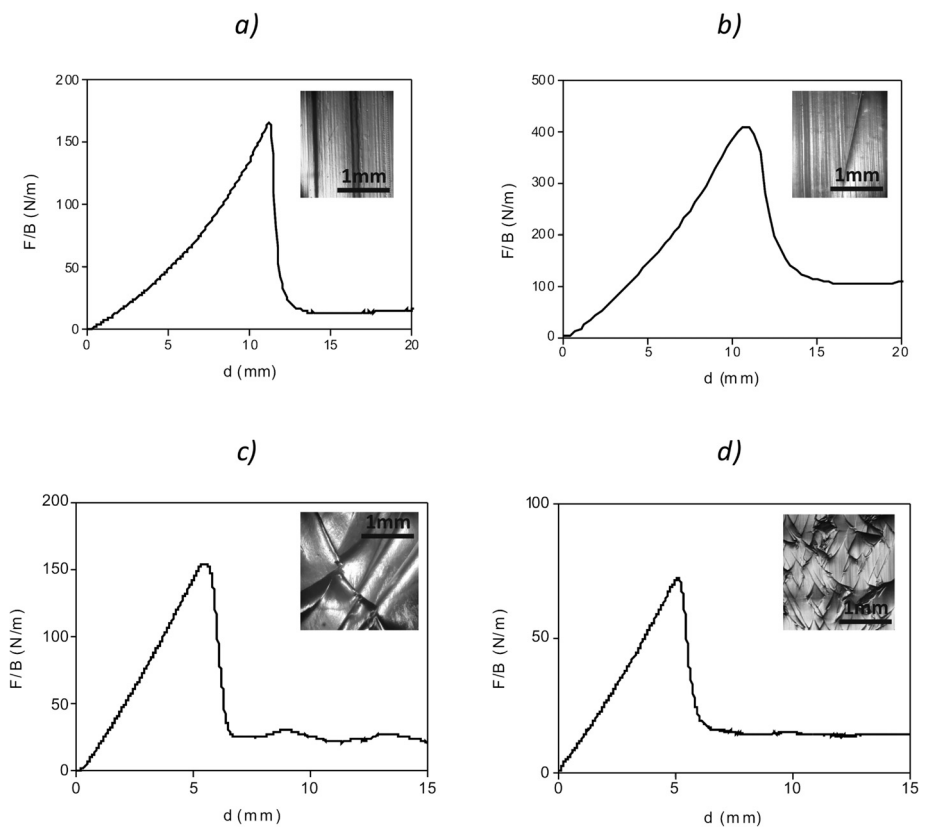

FIG. 8
Typical load–displacement curves obtained at different cutting rates for a given gel sample composition and wire diameter (GeBo-30, $d_w = 0.5$ mm).

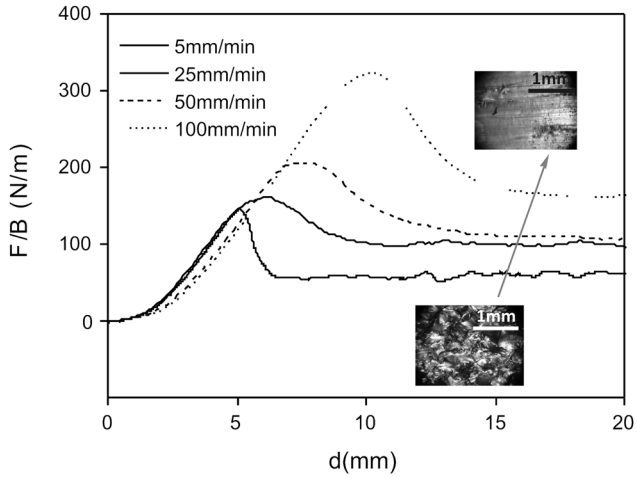

value [**Fig. 7(c)**]. The amplitude of the oscillations correlated well with the features of the steps: the smaller and more numerous the rhombus-like structures and the shorter the height of the steps, the smaller the amplitude of force oscillations [**Fig. 7(c)** and **7(d)**]. **Figure 8** shows that force–displacement oscillations decreased as the cutting rate increased, undergoing a transition from a fine rhombus-like structure at low rates to a striated pattern at high rates. Therefore, it is evident that oscillations are due to deflection of the crack front line.

Baumberger et al. [27] gave a consistent explanation of the crack propagation that yields a cross-hatched morphology in gelatin gels under mode I crack opening. A cross-hatched morphology is formed as a consequence of the emergence of a defect that first grows along the front direction. The crack front then becomes discontinuous and grows at different planes originating in the material, overhanging and leaving complementary steps on the crack surfaces. They attributed step

FIG. 9 Typical load–displacement curves obtained for cutting experiments with large crack path deflection: (a) PoGe-20, $V = 5$ mm/min, $d_w = 0.8$ mm (the optical microscopy image included shows the fracture surface morphology); (b) BoGe-10, $V = 100$ mm/min, $d_w = 0.8$ mm (the image included shows a side view of the two matching surfaces).

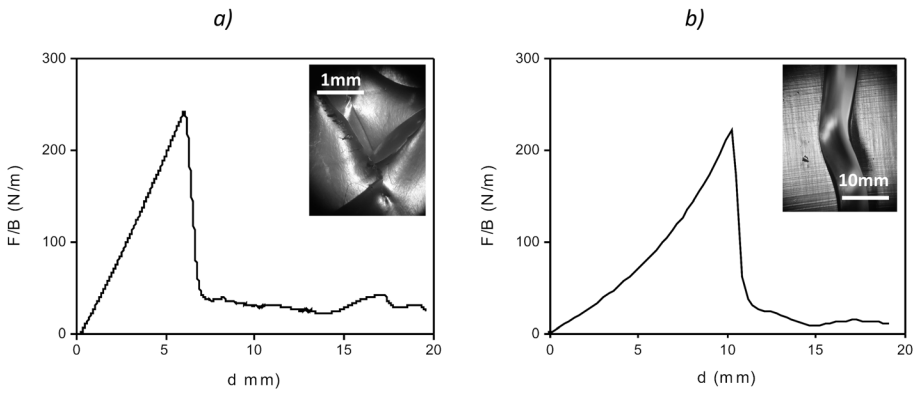

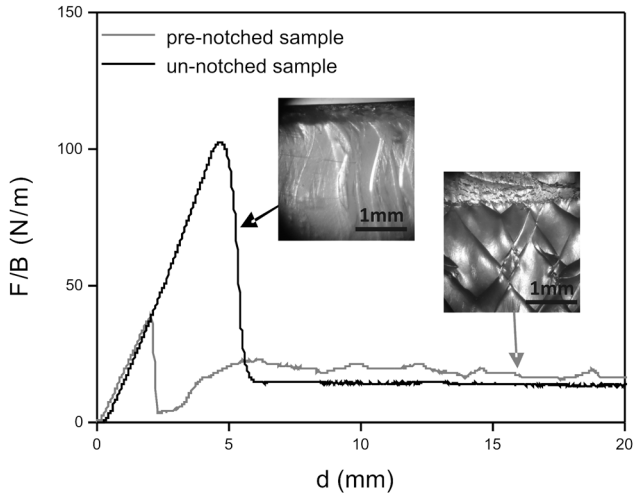

FIG. 10
Comparison of load–displacement curves obtained in cutting experiments of PoGe-20 at 5 mm/min and $d_w = 0.4$ using un-notched and prenotched samples.

nucleation to the randomness of the network structure of gelatin gels [27], which is composed of tough zones that are able to partially pin part of the crack front. The other part of the crack is delayed because it skirts the tough zone via out-of-plane deflection.

Abnormal force–displacement oscillations were registered when the fracture process occurred with no regular patterns or when only a few steps of large height developed (**Fig. 9**). Concomitantly, the load–displacement curves showed important deviations from a constant value during the cutting phase. This atypical behavior was observed in wire cutting experiments of PoGe-20 samples with low rates and large wire diameters [**Fig. 9(*a*)**] and for BoGe-10 samples at several rates and with large wire diameters [**Fig. 9(*b*)**].

The effect of using un-notched or prenotched samples is shown in **Fig. 10**. The presence of the prenotch changed the shape of the indentation part of the load–displacement curve. Because of the presence of a preexistent flaw, the large increase in force observed in the initial part of the experiment was practically eliminated. The prenotched sample stored less elastic energy during the initial stage and thus was less deformed than the un-notched sample.

The most important finding was that the presence of a prenotch was able to alter the fracture surface pattern and hence change the shape of the load–displacement curve in the steady-state cutting phase. In the example shown in **Fig. 10**, the fracture pattern changed from striated to rhombus-like, as revealed by optical microscopy of the post-mortem fracture surfaces and by the force-line trace oscillations. Moreover, the average value of the recorded cutting force was greater for the rhombus-like morphology than for the striated one. This can be explained by the greater crack path tortuosity of the rhombus-like pattern.

In cutting experiments in which un-notched samples developed rhombus-like fracture surface patterns, the propagation mode was unaltered by the incorporation of the prenotch, and no significant differences in the average cutting force or load oscillations were observed. These results are in agreement with those reported by

Baldi et al. [25] for PAA hydrogels. They preferred the use of prenotched samples because the variability in the initial part of the curves could be reduced with no differences in the steady-state value. However, our results show that this strategy could change the crack propagation pattern.

Another question then emerges about the wire cutting phenomenology: Why is the rhombus-like pattern promoted by a prenotch? Baumberger et al. [27] postulated that the development of the cross-hatched morphology needs nucleation and that there is a threshold value or critical crack propagation velocity (V_c) below which the structural noise due to randomness of the gel network is not strong enough for the step nucleation barrier to be overcome. Our results showed that the appearance of the rhombus-like pattern was related not only to the imposed cutting rate but also to the elastic energy stored in the specimen prior to crack propagation initiation (**Fig. 10**). It seems that the actual crack front velocity is greater when a large amount of stored elastic energy is released at crack initiation than when less deformed material is involved (prenotched samples). At high rates, the toughened zones are not able to arrest the crack front, and thus once initiated the crack propagates continuously without deflection during the rest of the experiment.

WIRE CUTTING PLOTS

Table 2 summarizes the results obtained after plotting the experimental cutting force per unit width (F_c/B) versus the wire diameter (d_w) and applying Eq 1 to fit the data. All data obtained for different cuts at each wire diameter were averaged and plotted with error bands. Then, they were linearly fitted according to Eq 1 using least squares and an instrumental weighting method. Data lying outside the 95 % confidence limits from the first best-fit line were eliminated from the analysis. The intercept values and regression coefficients listed in **Table 2** arose from a second linear fitting considering only valid data.

The following statements regarding the validity of the wire cutting methodology emerged from the analysis of **Table 2**.

A. The cutting method was not valid (i.e., a straight line was not observed) if:

- A transition between a rhombus-like to a striated pattern occurred with increasing wire diameter. This was the case when PoGe-20 was tested at 5 mm/min. Data did not follow an increasing linear trend with increasing wire diameter [**Fig. 11(a)**]. The use of prenotched samples was not able to induce the rhombus-like pattern in this situation. The cutting plot resembles the ones displayed by Baldi et al. for PAA hydrogels in which the fracture surface pattern changed with increasing wire diameter [11].
- The surface morphology was rhombus-like but abnormal, displaying few figures with large step heights, or the overall crack growth direction deviated from the wire advance direction (**Fig. 9**). This was the case for BoGe-10 samples tested at 5 mm/min [**Fig. 11(b)**], for which data appeared widely scattered.
- Severe damage with material pull-out appeared in the fracture surface. For this morphology, which was observed in BoGe-30 un-notched samples tested at 25 mm/min, the cutting forces registered—especially for large diameters—were greater than the expected tendency [**Fig. 11(c)**]. The use of prenotched samples reversed this situation, and the appearance of pull-out damage was shifted to the largest wire diameter ($d_w = 0.8$ mm), converting the situation to one of the type described next.

TABLE 2

Summary of results on application of the wire cutting method to prepared gelatin hydrogels.

		Cutting Rate, mm/min		
Sample	Method Details	5	25	100
BoGe-10	Validity of Eq 1 (R^2)	Invalid	Valid up to $d = 0.5$ mm (0.99527)	Valid up to $d = 0.6$ mm (0.99095)
	Surface morphology	Rhombus-like with large crack path deflection	Rhombus-like with transition to one or two rhombuses at large wire diameters	One or two oblique straight line defects
	Intercept value, N/m	–	1.4	7.2
BoGe-20	Validity of Eq 1 (R^2)	Valid up to $d = 0.6$ mm (0.93108)	Valid up to $d = 0.6$ mm (0.99293)	Valid up to $d = 0.6$ mm (0.96776)
	Surface morphology	Fine-size rhombus-like	Medium-size rhombus-like	One or two oblique straight line defects
	Intercept value, N/m	5.7	5.6	12.8
BoGe-30	Validity of Eq 1 (R^2)	Valid up to $d = 0.5$ mm (0.97575)	Valid up to $d = 0.5$ mm for prenotched samples (0.99983)	Valid (0.98801)
	Surface morphology	Fine-size rhombus-like with damage at large wire diameters	Large-size rhombus-like with damage at large wire diameters	One or two oblique straight line defects
	Intercept value, N/m	11	4.3	34.8
BoGe-10-GTA	Validity of Eq 1 (R^2)	Not tested	Valid (0.99029)	Not tested
	Surface morphology	Striated	Striated	Striated
	Intercept value, N/m	–	8.0	–
BoGe-20-Gly	Validity of Eq 1 (R^2)	Valid up to $d = 0.6$ mm (0.91587)	Valid (0.99301)	Not tested
	Surface morphology	Fine-size rhombus-like	Medium-size rhombus-like	Not tested
	Intercept value, N/m	7.2	7.0	–
PoGe-20	Validity of Eq 1 (R^2)	Invalid	Valid for prenotched samples (0.93596)	Valid (0.99896)
	Surface morphology	Transition from rhombus-like to striated with increasing wire diameter	Large-size rhombus-like	One or two oblique straight line defects
	Intercept value, N/m	–	18.0	17.2

B. The cutting method was valid for a limited range of wire diameters (i.e., a straight line was observed for wire diameters smaller than a critical value) if:

- The rhombus-like pattern remained practically unaltered while the wire diameter was increased up to the critical value. The use of wire diameters larger than this critical value led to smoother surface morphologies, and the load per unit width appeared to reach a plateau value. It has to be pointed out that this situation was the most frequently observed in the experiments (**Table 2**). Two representative cutting plots are shown in **Figs. 12(*a*)** and **12(*b*)**. It appeared that the fracture

FIG. 11 Plots of cutting force per unit width versus wire diameter. Experiments in which a straight line was not observed: (a) PoGe-20 (V = 5 mm/min); (b) BoGe-10 (V = 5 mm/min); (c) BoGe-30 (un-notched samples, V = 25 mm/min; the included optical microscopy image shows the fracture surface morphology).

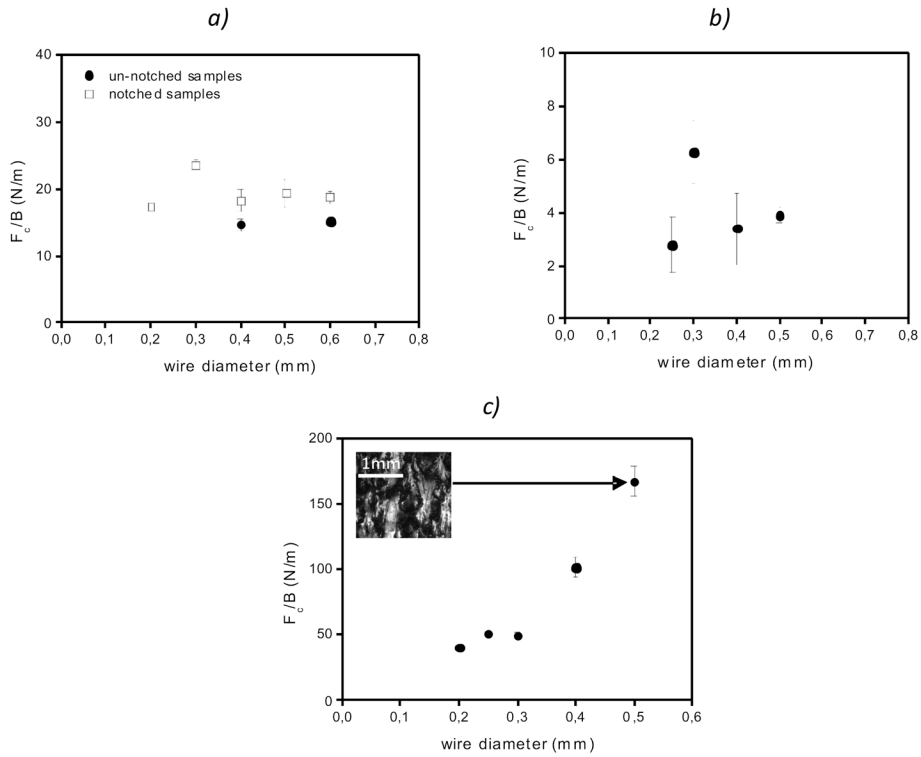

process lost self-similarity with large wire diameters. This effect can be related to the fact that the crack path tends to deflect to a lesser extent when large diameters are used; therefore the cutting force required in order to sustain propagation must be lower. It is shown in **Fig. 10** that for a given wire diameter, the rhombus-like pattern developed at greater cutting forces than the striated one.

- Material pull-out damage was shifted toward the largest wire diameters with the introduction of a prenotch in the samples. In these experiments, a rhombus-like pattern prevailed in the fracture surface instead of pull-out damage, as can be seen in the included optical micrographs in **Figs. 10(c)** and **11(c)**. This behavior was observed in tests carried out on BoGe-30 prenotched samples at 25 mm/min [**Fig. 12(c)**]. Note that the steady-state cutting force per unit width was less than that of the un-notched sample [**Fig. 11(c)**] consistent with the different morphologies that developed on the fracture surfaces.
  A change in the slope of the wire cutting plots was observed by Goh et al. in experiments on cheese samples [9]. They attributed the nonlinearity to a combined effect of a decrease in the strain rate with increasing wire diameter, which can result in a reduced value of the total cutting energy, and the appearance of secondary damage.

C. The cutting method was valid over the complete range of wire diameters tested (i.e., all data points fell on a straight line of fit) only if a striated morphology or one or two oblique line defects developed during crack propagation in

FIG. 12 Plots of cutting force per unit width versus wire diameter. Experiments in which a straight line was observed up to a critical wire diameter: (a) BoGe-10 (V = 25 mm/min); (b) BoGe-20 (V = 25 mm/min); (c) BoGe-30 (prenotched samples, V = 25 mm/min; the included optical microscopy image shows the fracture surface morphology).

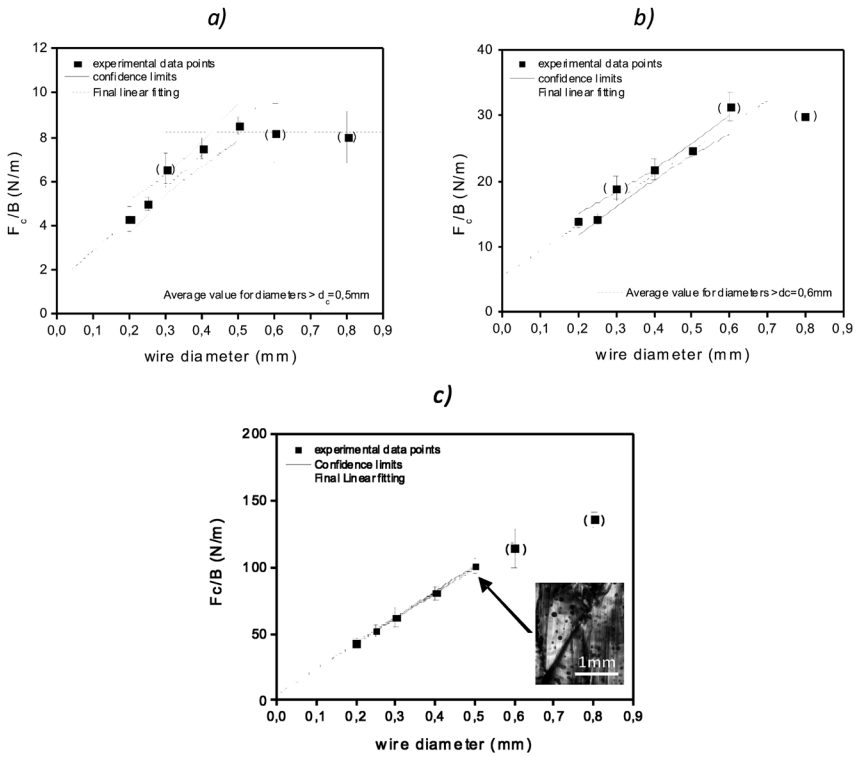

physical hydrogels, as in experiments carried out on stiff samples at 100 mm/min [**Figs. 13(*a*)** and **13(*b*)**].

One of the most important results was that the validity of Eq 1 might not be constrained only to physical gels, as judged by the wire cutting plot and regression coefficient obtained for GeBo-10-GTA experiments [**Fig. 13(c)**].

ANALYSIS OF INTERCEPT VALUES (G_C)

In previous studies employing other classes of soft materials [2,8–10], it was concluded that the wire cutting test can be used to measure the fracture toughness due to the similarities of the G_c values obtained from this test and those assessed via conventional fracture mechanics configurations. Results were in good agreement despite the hypothesis implicit in Eq 1 that a single crack propagation was violated [8].

In the present analysis, the intercept values reported in **Table 2** were considered as the fracture toughness values displayed by the prepared samples under different cutting rates.

Our results suggested that the fracture toughness of hydrogels is greater when a rhombus-like pattern develops, rather than a striated pattern, due to the greater crack tortuosity of the former mechanism. This resembles the increase in toughness observed in brittle materials such as polymeric matrices and cements as a result of the crack path deflection caused by inclusions [29,30].

FIG. 13 Plots of cutting force per unit width versus wire diameter. Experiments in which a straight line was observed in the complete wire diameter range tested: (a) BoGe-30 (V = 100 mm/min); (b) PoGe-20 (V = 100 mm/min); (c) BoGe-10-GTA (V = 25 mm/min).

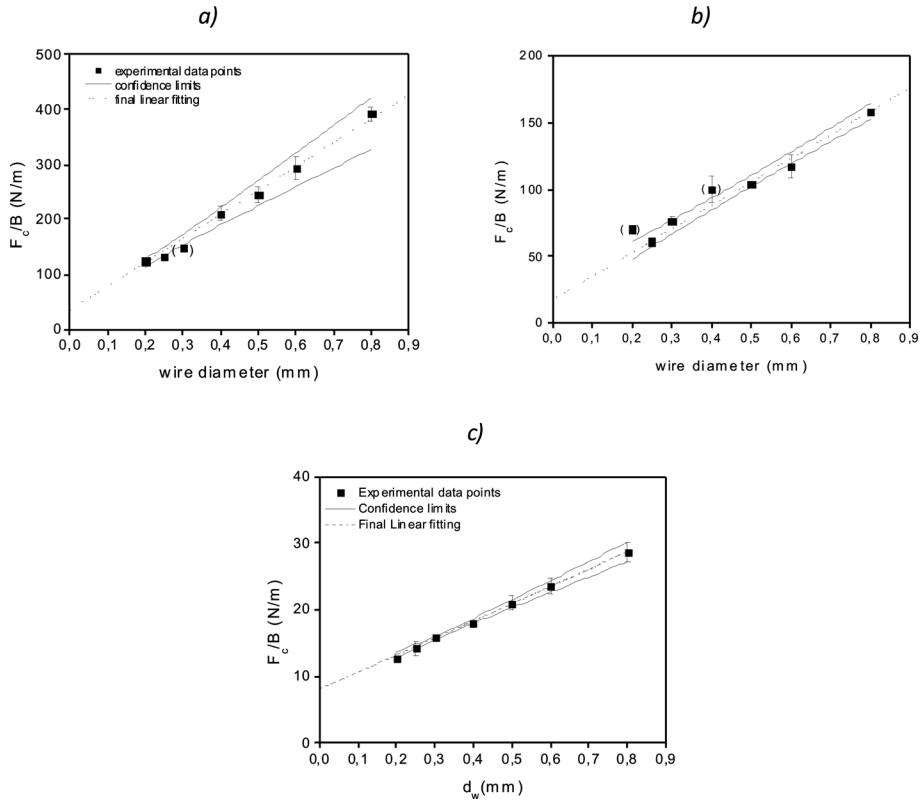

Baumberger et al. [5] proposed that fracture in physical gels takes place via a viscoplastic disentanglement process. It occurs via scissionless chain pull-out with energy dissipation mainly due to viscous drag. They demonstrated that the energy release rate of gelatin gels G_c depends on the viscosity (η) and crack velocity (V), as [5]

$$G_c = G_0 + \Gamma \eta V \tag{2}$$

where:

Γ = rate sensitivity parameter on the order of 10^6 proportional to gel stiffness, and

G_0 = quasi-static toughness parameter.

Equation 2 predicts that the fracture toughness of gelatin hydrogels will increase with increasing crack propagation rate, solvent viscosity, and gelatin concentration. Equation 2 was derived from the analysis of G_c values measured at crack velocities greater than the critical value (V_c), that is, at crack propagation rates at which striated fracture surfaces developed.

The expected evolution of fracture toughness parameters with cutting rate given by Eq 2 was not observed in gel samples that underwent a fracture surface pattern

transition from type I or II to type III with decreasing cutting rate. Note that G_c values remained almost constant for BoGe-20 and BoGe-20-Gly samples tested at 5 and 25 mm/min and for PoGe-20 samples at 25 and 100 mm/min. We attributed this effect to the combination of an inherent increase in crack propagation rate and a concomitant reduction in crack tortuosity with increasing cutting rate. In contrast, in gel samples that developed type I and type II morphologies, the determined G_c values were in excellent agreement with Eq 2.

In order to compare G_c values and analyze the effects of gelatin concentration, gelatin source, solvent viscosity, and crosslinking type, data obtained only when the same fracture surface pattern developed were considered.

The effect of bovine gelatin concentration was evaluated based on results obtained at 100 mm/min for GeBo-10, GeBo-20, and GeBo-30 samples in which type II morphology developed. Fracture toughness increased with increasing gelatin concentration and G_c values followed a power law relationship with an exponent equal to 2. A similar dependence was displayed by the gel strength values (**Table 1**), indicating that the stiffer the gel is, the tougher it is.

The effect of gelatin source (bovine or porcine) on G_c was analyzed based on results obtained at 100 mm/min for GeBo-20 and PoGe-20 samples. At this cutting rate, both samples exhibited type II morphology, but porcine gelatin yielded tougher hydrogels than bovine gelatin. The PoGe-20 sample was stiffer than the BoGe-20 sample, but the difference in toughness was twice as large as the difference in stiffness.

The incorporation of glycerol did not alter the developed fracture pattern in bovine gelatin gels, but it increased the fracture toughness, as revealed by the G_c values determined at 5 and 25 mm/min for GeBo-20 and GeBo-20-Gly. This is in agreement with Eq 2, as the incorporation of glycerol increased the solvent viscosity, and it is also in agreement with previous findings [5].

The fracture toughness parameter of the chemically crosslinked hydrogel (BoGe-10-GTA) was about six-fold greater than that of the physical hydrogel (BoGe-10), despite the fact that the crack tortuosity of the former was lower. The increase in toughness might be due to scission of stretched chains in crosslinked gels rather than chain pull-out in physical gels [5].

Final Remarks

The experimental work and analysis performed in this study on gelatin-based hydrogels contributed to the elucidation of some of the conditions that need to be fulfilled in order for the wire cutting method to be applicable in evaluations of the fracture toughness of soft materials, especially hydrogels.

The validity of Eq 1 is in part related to the development of a unique fracture surface morphology for all the wire diameters (type I and II or type III morphologies) used in the experiments. This condition is hard to meet in hydrogels that can undergo different fracture patterns depending on the crack propagation velocity.

As a transition from rhombus-like to striated morphology occurs with increasing cutting rate, the nonlinearity in the wire cutting plots may arise from the existence of a crack path deflection toughening mechanism at small wire diameters that disappears at large wire diameters.

Other effects such as adhesion between wire and sample and abnormal crack path deflection due to excessive bending of very soft samples during the indentation phase also yield nonlinear wire cutting plots.

The wire diameter range used also must satisfy the development of a unique fracture surface morphology. But indeed, the smallest possible wire diameter range is recommended in order to obtain accurate intercept values. However, thin wires are difficult to keep taut when being used with hydrogels of a certain stiffness.

The validity of Eq 1 appears not to be constrained to physical hydrogels. It seems that in experiments by Baldi et al. on PAA hydrogels [11], the method was invalid because of evident changes in the fracture surface morphology, rather than the chemical crosslinked character of the gels as previously thought.

It appears that the actual crack propagation velocity at the onset of crack initiation, which determines the fracture surface morphology, depends on the elastic energy stored in the sample during the indentation phase. The stored energy is difficult to control in this test configuration because it depends on the inherent flaws or structural defects that nucleate the crack.

Given the simplicity of the wire cutting method, further work is encouraged in other classes of soft materials to explore the validation limits of the technique.

ACKNOWLEDGMENTS

The writers thank CONICET and MINCYT from Argentina for the financial support of this work.

References

[1] Suo, Z., "Fracture of Gels: A Field where Mechanics Meets Chemistry," http://imechanica.org/node/13088 (Last accessed 6 Dec 2013).

[2] Kamyab, I., Chakrabarti, S., and Williams, J. G., "Cutting Cheese With Wire," *J. Mater. Sci.*, Vol. 33, 1998, pp. 2763–2770.

[3] Gdoutos, E. E., Daniel, I. M., and Schubel, P., "Fracture Mechanics of Rubber," *Facta Universitatis, Series Mechanics, Automatic Control and Robotics*, Vol. 3, No. 13, 2003, pp. 497–510.

[4] Tanaka, Y., Kuwabara, R., Na, Y. H., Kurokawa, T., Gong, J. P., and Osada, Y., "Determination of the Fracture Energy of High Strength Double Network Hydrogels," *J. Phys. Chem. B*, Vol. 109, 2005, pp. 11559–11562.

[5] Baumberger, T., Caroli, C., and Martina, D., "Fracture of a Biopolymer Gel as a Viscoplastic Disentanglement Process," *Eur. Phys. J.*, Vol. E21, 2006, pp. 81–89.

[6] Patel, Y., Blackman, B. R. K., and Williams, J. G., "Determining Fracture Toughness from Cutting Tests on Polymers," *Eng. Fract. Mech.*, Vol. 76, 2009, pp. 2711–2730.

[7] Kwon, H. J., Rogalsky, A. D., and Kim, D.-W., "On the Measurement of Fracture Toughness of Soft Biogels," *Polym. Eng. Sci.*, Vol. 51, No. 6, 2011, pp. 1–9.

[8] Goh, S. M., 2002, "An Engineering Approach to Food Texture Studies," PhD thesis, Imperial College of Science, Technology and Medicine, University of London, London, UK.

[9] Goh, S. M., Charalmbides, M. N., and Willimas, J. G., "On the Mechanics of Wire Cutting of Cheese," *Eng. Fract. Mech.*, Vol. 72, 2005, pp. 931–946.

[10] Gamonpilas, C., Charambides, M. N., and Williams, J. G., "Determination of Large Deformation and Fracture Behavior of Starch Gels from Conventional and Wire Cutting Experiments," *J. Mater. Sci.*, Vol. 44, 2009, pp. 4976–4986.

[11] Baldi, F., Bignotti, F., Peroni, I., Agnelli, S., and Riccò, T., "On the Measurement of the Fracture Resistance of Polyacrylamide Hydrogels by Wire Cutting Tests," *Polym. Test.*, Vol. 31, 2012, pp. 455–465.

[12] Gómez-Guillén, M. C., Giménez, B., López-Caballero, M. E., and Montero, M. P., "Functional and Bioactive Properties of Collagen and Gelatin from Alternative Sources: A Review," *Food Hydrocolloids*, Vol. 25, 2011, pp. 1813–1827.

[13] Schrieber, R. and Gareis, H., *Gelatine Handbook*, Wiley-VCH GmbH & Co, Weinhem, Germany, 2007.

[14] Fu, Y., Xu, K., Zheng, X., Giacomin, A. J., Mix, A. W., and Kao, W. J., "3D Cell Entrapment in Crosslinked Thiolated Gelatin-poly(ethylene glycol) Diacrylate Hydrogels," *Biomaterials*, Vol. 33, 2012, pp. 48–58.

[15] Young, S., Wong, M., Tabata, Y., and Mikos, A. G., "Review. Gelatin as a Delivery Vehicle for the Controlled Release of Bioactive Molecules," *J. Controlled Release*, Vol. 109, 2005, pp. 256–274.

[16] Kwon, J. and Subhash, G., "Compressive Strain Rate Sensitivity of Ballistic Gelatin," *J. Biomech.*, Vol. 43, No. 3, 2010, pp. 420–425.

[17] Bigi, A., Cojazzi, G., Panzavolta, S., Rubini, K., and Roveri, N., "Mechanical and Thermal Properties of Gelatin Films at Different Degrees of Glutaraldehyde Crosslinking," *Biomaterials*, Vol. 22, 2001, pp. 763–768.

[18] Saarai, A., Kasparkova, V., Sedlacek, T., and Saha, P., "On the Development and Characterization of Crosslinked Sodium Alginate/Gelatin Hydrogels," *J. Mech. Behav. Biomed. Mater.*, Vol. 18, 2013, pp. 152–166.

[19] Yan, M., Li, B., Zhao, X., and Yi, J., "Physicomechanical Properties of Gelatin Gels from Walleye Pollock (*Theragra chalcogramma*) Skin Crosslinked by Gallic Acid and Rutin," *Food Hydrocolloids*, Vol. 25, 2011, pp. 907–914.

[20] Fernández Díaz, M. D., Montero, P., and Gómez Guillén, M. C., "Gel Properties of Collagens from Skins of Cod (*Gadus morhua*) and Hake (*Merluccius merluccius*) and Their Modification by the Conenhancers Magnesium Sulphate, Glycerol and Transglutaminase," *Food Chem.*, Vol. 74, 2001, pp. 161–167.

[21] Czerner, M., Fasce, L. A., and Frontini, P. M., "Deformation and Fracture of Mammalian Protein Based Gels," *Proceedings of the 5th International Conference PMI2012*, Ghent, Belgium, Sept. 12–14, 2012, Centre for Polymer and Material Technologies CPMT of University College Ghent (Belgium) and the Institute of Polymers and Composites IPC of University of Minho (Portugal), pp. 230–237.

[22] Groot, R. D., Bot, A., and Agterof, W. G. M., "Molecular Theory of Strain Hardening of a Polymer Gel: Application to Gelatin," *J. Chem. Phys.*, Vol. 104, No. 22, 1996, pp. 9202–9219.

[23] Atkins, T., *The Science and Engineering of Cutting: The Mechanics and Processes of Separating and Puncturing Biomaterials, Metals and Non-metals*, Butterworth-Heinemann, Stoneham, MA, 2009, pp. 300–306.

[24] Usta, M., Piech, D. L., MacCrone, R. K., and Hillig, W. B., "Behavior and Properties of Neat and Filled Gelatins," *Biomaterials*, Vol. 24, 2003, pp. 165–172.

[25] Baldi, F., Bignotti, F., and Riccò, T., "Determination of the Fracture Resistance of Polymer Gels via Cutting With Wire," *Proceedings of the 12th International Conference on Fracture, ICF-12*, Ottawa, ON, Canada, July 12–17, 2009, National Research Council Canada, Ottawa, ON, Canada, pp. 1–9.

[26] Tanaka, Y., Fukao, K., Miyamoto, Y., Nakazawa, H., and Sekimoto, K., "Regular Patterns on Fracture Surfaces of Polymer Gels," *J. Phys. Soc. Jpn.*, Vol. 65, No. 8, 1996, pp. 2349–2352.

[27] Baumberger, T., Caroli, C., Martina, D., and Ronsin, O., "Magic Angles and Cross-hatching Instability in Hydrogel Fracture," *Phys. Rev. Lett.*, Vol. 100, 2008, pp. 178303–178307.

[28] Gent, A. N. and Pulford, C. T. R., "Micromechanics of Fracture in Elastomers," *J. Mater. Sci.*, Vol. 19, 1984, pp. 3612–3619.

[29] Pearson, R. A. and Yee, A. F., "Toughening Mechanisms in Thermoplastic-modified Epoxies: 1. Modification Using Poly(phenylene Oxide)," *Polymer*, Vol. 34, No. 17, 1993, pp. 3658–3670.

[30] Abell, A. B. and Lange, D. A., "The Role of Crack Deflection in Toughening of Cement-based Material," *International Symposium Proceedings, Brittle Matrix Composites 5*, A. M. Brandt, V. C. Li, and L. H. Marshall, Eds., BIGRAF, Warsaw, Poland, 1997, pp. 241–250.